Efficient topology design for district heating networks with multiple geographically distributed sources and limited supply capacities

Laura Kuper[a,b,], Michael Metzger[a], Paul Stursberg[a], Lukas Glotzbach[c] and Stefan Niessen[a,b]*

[a] *Siemens AG - Foundational Technology - Sustainable Energy and Infrastructure, Munich/Erlangen, Germany,*
[b] *TU Darmstadt - Technology and Economics of Multimodal Energy Systems, Darmstadt, Germany,*
[c] *GGEW - Gruppen-Gas- und Elektrizitätswerk Bergstraße Aktiengesellschaft, Bensheim, Germany,*
** laura.kuper@siemens.com, CA*

Abstract:

Decarbonizing urban heating requires the integration of sustainable heat sources into district heating networks (DHN). Since these sources, like large-scale air-source heat pumps, ambient water systems, or waste heat recovery are spatially bound and capacity-limited, networks must transition from centralized supply to multi-source systems. However, designing optimal topologies for such systems is computationally intensive, limiting existing approaches to small neighborhoods or two to three potential sources. This paper presents a novel, computationally efficient optimization framework based on a Prize-Collecting Steiner Tree (PCST) algorithm to address these scaling challenges.

The framework identifies the most profitable design by optimizing topologies for source subsets, using a golden ratio search. Within this search, single-source PCSTs are solved and merged into a joint topology. The joint topology is evaluated using hourly merit-order dispatch. The resulting subset topologies are combined into candidate topologies, which may consist of a single connected network or multiple independent subnetworks. A final comparison of all candidates identifies the most profitable overall design.

Due to the computational efficiency of the PCST optimization, the method scales to city-wide planning as highlighted in this work by a case study, featuring seven potential heat sources and 6,200 buildings. Results demonstrate that the framework successfully identifies profitable multi-source configurations, favoring synergies between sources to overcome individual capacity limitations. Additionally, the approach provides insights into the feasibility of various network layouts and the adjustments required to render alternative potential configurations profitable.

Keywords:

Computational efficiency; District heating; Graph algorithms; Optimization; Renewable heat sources.

1. Introduction

District heating networks (DHN) serve as a central element in the decarbonization of urban energy systems [1], enabling the integration of sustainable heat sources and enhancing energy efficiency [2]. Sustainable sources are typically distributed and limited in capacity by physical availability, spatial requirements, regulatory restrictions and the accessibility of the source for heat suppliers. Consequently, future DHNs will increasingly rely on multiple heat generation units distributed across the urban environment. However, the location of the sources directly influences possible network topology. Hence, piping network topology design must integrate source selection with route planning and the choice of which consumers to connect.

Existing literature on multi-source DHN design usually focuses on selected aspects to balance scale and granularity. Research regarding potential analyses often adopts a spatially aggregated demand perspective, which identifies connections between demand clusters but lacks the granularity required for street-level pipe

routing [3]. Studies that do focus on individual sources and consumers often address only neighborhood-scale and simplify the topology design to a limited number of predefined connections. For instance, Marty et al. optimized a geothermal source for only seven potential consumers [4]. Other neighborhood-scale models integrate multiple generation units with up to approximately 30 buildings [5,6]. At the district scale with a few hundred consumers, studies by Wack [7], Sollich [8] and Ceruti [9] have addressed up to two sources, with Sollich and Ceruti also incorporating storage considerations. However, these approaches do not scale to city-wide planning with numerous potential sources and source locations.

The limitations in scaling the existing models to larger districts and more sources are primarily rooted in the high computational complexity of the underlying optimization problem. While optimizing single-source topologies is already inherently complex due to the large number of binary decision variables involved [10], the inclusion of source selection adds another layer of complexity. As the number of potential sources increases, the underlying search space expands, causing computation times to scale accordingly [9]. Furthermore, research by Wack [7] and Ceruti [9] indicates that multi-source design necessitates the consideration of multiple load cases from different seasons. While optimization based on a single load case generally results in isolated subnetworks for each source, interconnected topologies are typically found to be optimal under realistic operating conditions involving multiple load cases [7,9]. Since the inclusion of multiple load cases also increases the computational complexity [9,11], the combined effect of multiple load cases and an increasing number of potential sources makes the optimization with more than two or three sources prohibitively expensive, even at the district scale with a few hundred consumers. Consequently, optimizing DHN topologies for larger districts while accommodating more than two or three sources remains a bottleneck in existing optimization frameworks.

To address these computational challenges, this work presents a novel, computationally efficient optimization framework for multi-source DHN. By utilizing a graph algorithm for the Prize-Collecting Steiner Tree (PCST) problem, the proposed framework is shown to be capable of:

- Simultaneous consideration of at least seven potential heat sources.
- Scaling to large districts or entire cities with multiple thousand potential consumers
- profiles in hourly resolution.
- Selecting optimal source combinations and the identification of resulting subnetworks.

The scope of this work is focused on the topological layout and source selection. Detailed calculation of pipe diameters and the design of thermal storage systems are excluded from the current analysis and should be performed based on the selected layout at a later planning stage. The work considers linearized investment costs, potentially overlooking economies of scale for larger units.

2. Methodology

The primary objective of the proposed framework is to identify a network topology that maximizes economic profitability by balancing heat revenues against generation and infrastructure costs, while considering multiple available heat sources. In this context, topology design targets the decision-making process of source selection, consumer connectivity, and the routing of the piping network. The topology is thereby the set of pipes connecting consumer and sources and may consist of a single interconnected system or several independent subnetworks, depending on the spatial distribution of sources and demand.

Next to the location of the sources, several techno-economic source parameters influence the multi-source topology design. These parameters include 1) the available heat generation capacity, limiting network dimension, 2) heat generation costs, influencing source attractiveness and profitability of the network, and 3) construction cost, affecting viability of network configurations. Furthermore, the decision between constructing a single interconnected network or multiple subnetworks must be addressed.

The presented framework builds upon two pillars: 1) The generation of candidate topologies, by building upon a graph-based approach derived from the Prize-Collecting Steiner Tree (PCST) approach for single-source topology design [10] to efficiently identify promising topologies for various combinations of sources, and 2) the assessment and comparison of candidate topologies to select the best-performing topology based on economic performance across hourly load cases.

In the following subsection, we provide a high-level overview of the framework's workflow, formalize the objective function used for topology assessment, detail the optimization of source combinations to generate subset topologies and describe the composition and evaluation of candidate topologies.

2.1. Overall framework

The proposed framework identifies the most profitable multi-source DHN topology while maintaining computational efficiency by combining fast graph-based optimization with systematic selection of promising source configurations. The framework comprises five stages: graph construction, initialization and clustering, optimization of source combinations, candidate composition, and final assessment (Fig 1).

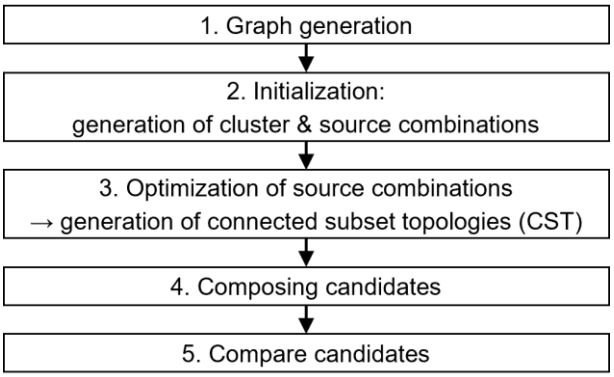

Figure 1. *Optimization framework procedure: Multi-source district heating network (DHN) topologies are generated over multiple stages and finally assesed and compared.*

An initial undirected **graph** $G = (V, E)$ is constructed using georeferenced data for buildings, potential heat sources, and potential pipe routes. The nodes V represent potential consumers, connection junctions, and the heat sources. The edges E represent potential pipe segments.

To minimize computational effort, the optimization process is **initialized** by determining the 'upper bound' network for all sources together. Each source is optimized individually using the PCST algorithm under ideal conditions, assuming no capacity limits and the lowest variable generation costs of any source, regardless of whether it is the currently optimized source to find the best-case topology. The resulting single-source topologies are joined to identify the maximum theoretical extent of the multi-source topology. All sources that share a connected subnetwork in the joint topology are grouped into a **cluster**. Since sources in different clusters will not share a subnetwork in any feasible solution, this step allows the framework to pre-filter valid source combinations, potentially reducing the number of combinations to be analyzed in subsequent steps.

For each identified cluster, the framework considers every possible **subset of sources**, also referred to as source combination, to determine whether these sources can jointly supply a connected (sub-)network and what the optimal topology of that network would be. If a source combination can jointly supply a connected network, this network is referred to as a **connected subset topology (CST)**.

In the next stage, individual CSTs are assembled into **candidate topologies**. A candidate topology represents a complete potential network design for the district or city and may consist of one or multiple unconnected subnetworks. Formally, a candidate is defined by a partition of a subset of sources, where each block of the partition corresponds to a CST.

The final step assesses the candidate topologies. Each candidate is evaluated against the objective function (Section 2.2) considering hourly load and generation profiles to account for seasonal variations. By comparing the economic performance of all candidates, the framework identifies the overall best-performing topology for the given urban area.

2.2. Economic assessment and objective function

The objective function defined in this section serves a dual purpose: it acts as the optimization criterion for generating individual CSTs in stage 3 and provides the basis for the comparison of candidate topologies in stage 5. To account for the necessity of multiple load cases discussed in Section 1 and for not only seasonal but also daily fluctuations, all calculations are performed at an hourly resolution

$h = \{1, \dots, 8760\}$. All topologies are assessed based on their annual profit Π, using equivalent annual annuities to ensure comparability between investments with different lifetimes and annual cash flows:

$$\begin{aligned} \Pi &= R_{\text{sale}} - \sum_{s \in S} (OPEX_s + I_s) - I_{\text{topo}} \\ &= p \cdot \sum_{h=0}^{8760} Q_{\text{cons}}(h) - \sum_{s \in S} \left(c_s \cdot \sum_{h=0}^{8760} Q_{\text{gen},s}(h) + I_{\text{base},s} \right) - l_{\text{topo}} \cdot \kappa_{\text{topo}} \end{aligned} \tag{1}$$

Here, R_{sale} denotes the annual heat sale revenues, $OPEX_s$ and I_s are the annualized operating and investment costs of each source s, and I_{topo} represents the annualized costs for pipe connection construction. Operating costs for the network infrastructure are assumed to be negligible compared to the other cost terms and therefore not considered.

The sales revenue R_{sale} is derived from the hourly heat demand aggregated over all consumers $Q_{\text{cons}}(h)$ multiplied with the consumer heat price p. While the approach allows a varying p for different consumers, we assume the same p for all consumers for simplicity.

The annualized source costs $OPEX_s$ and I_s are restructured into fixed base costs $I_{\text{base},s}$ and variable costs, which depend on the hourly generated heat $Q_{\text{gen},s}(h)$. The variable cost parameter c_s includes generation costs $c_{\text{gen},s}$, maintenance costs $c_{\text{O\&M},s}$ and capacity-dependent investment costs i_s:

$$c_s = OPEX_s + i_s = c_{\text{gen},s} + c_{\text{O\&M},s} + i_s \tag{2}$$

To determine the heat contribution of each source, the dispatch is prioritized based on a merit order principle. Sources are sorted into a set $S = \{1, \dots, N\}$ such that $c_s \leq c_{s+1}$. Based on this order, the hourly dispatch $Q_{\text{gen},s}(h)$ is determined by the residual heat generation and limited by the source's hourly capacity $Q_{\text{gen},s,\max}(h)$. This dispatch ensures that the most cost-effective sources–considering both operation and investment–are utilized first:

$$Q_{\text{gen},s}(h) = \max\left(0, \min\left(Q_{\text{gen},s,\max}(h)\,, Q_{\text{gen}}(h) - \sum_{k=1}^{s-1} Q_{\text{gen},k,\max}\right)\right) \tag{3}$$

Following prior findings [10], we assume that network heat losses can be represented by a system-wide parameter. The heat generation $Q_{\text{gen}}(h)$ thus compensates for losses via the network efficiency η_{topo}:

$$Q_{\text{gen}}(h) = Q_{\text{cons}}(h) \cdot \frac{1}{\eta_{\text{topo}}} \tag{4}$$

Furthermore, prior findings [10] have shown that diameters can be disregarded during the topology optimization phase as they have a negligible impact on the optimal layout compared to spatial routing. Consequently, the annualized piping costs I_{topo} depend solely on the total network length l_{topo} and the annualized construction cost per meter κ_{topo}.

2.3. Optimization of source combinations

This section presents the methodology developed to derive the optimal topology for a given combination of heat sources regarding the introduced objective. The objective is to determine whether the source combination can jointly supply a profitable connected network and, if so, identify the topology that maximizes annual profit Π. The method consists of three main elements: The extension of the PCST approach to multi-source configurations, a value scaling to control the network extent and a golden ratio search to identify the profit-maximizing network extent.

2.3.1 PCST formulation and multi-source integration

The framework builds upon the formulation of DHN design as a rooted PCST problem [10]. Based on the graph representation of the district $G = (V, E)$, the PCST algorithm identifies a subgraph $G' = (V', E')$ that maximizes the profit by balancing connected node values $values_v$ against edge expenditures $expenditure_e$:

$$\max\left(\sum_{v\in V'} value_v - \sum_{e\in E'} expenditure_e\right) \tag{5}$$

In the rooted PCST, one specific node in G is designated as the root. This root is always part of G' and can be interpreted as the heat source. To account for multiple heat sources, the PCST algorithm is executed N_{combi} times–once for each heat source s in the current combination S_{combi}. Each s is treated as the root once, yielding N_{combi} individual subgraphs $G_s' = (V_s', E_s')$. The union of these subgraphs forms the joint graph G'_{joint}:

$$G'_{\text{joint}} = \left(V'_{\text{joint}}, E'_{\text{joint}}\right) = \left(\bigcup_{s=1}^{N_{\text{combi}}} V_s', \bigcup_{s=1}^{N_{\text{combi}}} E_S'\right) \tag{6}$$

In each single-source PCST, $expenditure_e$ represents the annualized construction cost $I_{\text{topo},e}$ of edge e, which depends on the edge length. The base investment cost $I_{\text{base},s}$ in Eq. (1) acts as a constant offset for the objective. Since this offset does not influence the optimal topology, it is excluded from the PCST optimization and only considered during the final candidate evaluation in Section 2.4.

The node values $value_v$ represent the potential gross profit from connecting consumer v, calculated as the difference between sale revenues and the variable source cost per consumer node. While revenues depend directly on the consumer heat demand $Q_{\text{cons},v}(h)$, the generation costs are linked to this demand via the network efficiency η_{topo} as derived in Eq. (4):

$$value_v = \left(p - c_{\text{const}} \cdot \frac{1}{\eta_{\text{topo}}}\right) \cdot \sum_{h=0}^{8760} Q_{\text{cons},v}(h) \tag{7}$$

The reference cost c_{const} is defined as the minimum variable cost among all sources within the specific combination. By keeping c_{const} constant over all single-source PCSTs regardless of the current root, we obtain a best-case topology. This approach assumes–similar as in initialization stage–that all sources can supply heat at the cost of the most economical source.

2.3.2 Golden ratio search for profit maximization using α scaling

However, the effective average variable source cost for a network supplied by multiple sources depends on the source dispatch (Eq. (3)). Consequently, c_{const} typically underestimates the effective costs. To compensate for this, we introduce a scaling parameter $\alpha \leq 1$ to modify the node values:

$$value_v(\alpha) = \alpha \cdot \left(p - c_{\text{const}} \cdot \frac{1}{\eta_{\text{topo}}}\right) \cdot \sum_{h=0}^{8760} Q_{\text{cons},v}(h) \tag{8}$$

While $\alpha = 1$ represents the idealized case of minimum variable costs, decreasing α simulates the effect of rising variable costs, leading to smaller networks. If we evaluate the actual profit Π (Eq. (1)) according to the merit order dispatch for different values of α, we obtain the relationship illustrated in Fig 2. This scaling approach, inspired by Johnson's work on modified PCST problems [12], allows to explore the solution space of possible network topologies for a source combination to identify the profit-maximizing CST.

In addition to profit maximization, the optimization of a source combination must adhere to two constraints:

- Connectivity as lower bound: The joint graph G'_{joint} must form a single connected component. This is required because the use of a single scaling factor α assumes a shared cost structure across the network. If a reduction in α leads to fragmented sub-networks or isolated sources, these components would instead operate with individual costs based on their connected sources. Such fragmented configurations are explicitly addressed through the candidate composition described in Section 2.4.
- Capacity as upper bound: The total connected hourly demand must not exceed the combined hourly capacity of all sources in the source combination at any time step.

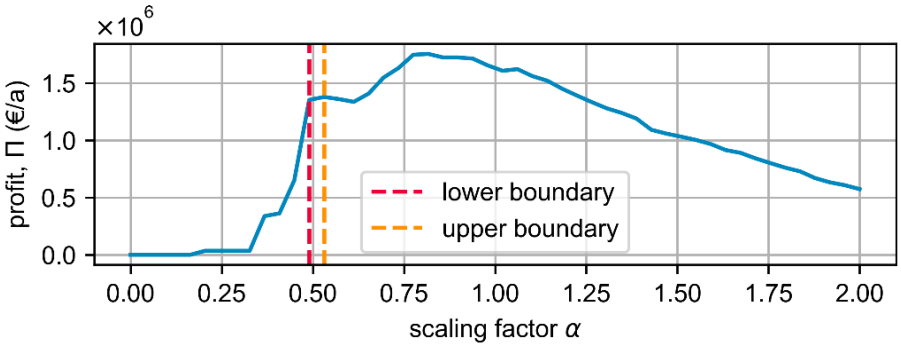

Figure 2. *Profit as a function of α. The maximum profit is achieved at $\alpha \approx 0.8 < 1$. The feasible region is bounded below by network fragmentation (red dashed line), and above by the sum of source capacities (yellow dashed line). The optimal feasible solution is at $\alpha \approx 0.55$, at the upper edge of the feasible region.*

To identify the optimal scaling factor α^* that maximizes the annual profit Π under the constraints, we apply a golden ratio search algorithm [13] extended to account for the constraints. This golden ratio search is designed for the optimization of unimodal functions, requiring a single local maximum within the search interval. As illustrated by Fig 2, $\Pi(\alpha)$ follows largely unimodal behavior. Despite minor spikes caused by the discrete nature of the topology changes, the global behavior justifies the application of the algorithm. The search algorithm iteratively narrows an initial interval $[\alpha_{\min}, \alpha_{\max}] = [0,1]$ by evaluating two sampling points α_1 and α_2 defined by the golden ratio $\phi \approx 1.618$:

$$\alpha_1 = \alpha_{\max} - \frac{\alpha_{\max} - \alpha_{\min}}{\phi}, \qquad \alpha_2 = \alpha_{\min} + \frac{\alpha_{\max} - \alpha_{\min}}{\phi} \tag{9}$$

In each step of the algorithm, G'_{joint} and the resulting profit $\Pi(\alpha)$ are calculated for each sampling point. To integrate the constraints into the search process, we define an evaluated profit $\Pi_{\text{eval}}(\alpha)$. If a sampling point violates any constraint, $\Pi_{\text{eval}}(\alpha)$ is penalized using a 'Big-M' approach (e.g. $M = 10^9$):

$$\Pi_{\text{eval}}(\alpha) = \begin{cases} \Pi(\alpha) & \text{if feasible} \\ -M & \text{if infeasible} \end{cases} \tag{10}$$

This 'Big-M' approach ensures that the search treats infeasible regions as global minima, effectively steering the search interval toward the feasible range of α. The sampling point yielding the lower profit $\Pi_{\text{eval}}(\alpha)$ replaces an interval boundary such that the other sampling point stays within the interval. Utilizing the golden ratio to determine the sampling points allows for the reuse of the sampling point from the preceding step that stays in the interval in the next iteration, requiring only one new PCST evaluation per iteration.

The iteration process terminates when the relative difference in Π between the last four feasible sampling points falls below a defined threshold, if a sampling point violates both constraints simultaneously, indicating that no feasible solution exists, or when a maximum number of iterations is reached. The optimization is performed for each source combination. If a feasible solution is found, the resulting topology is designated as the CST of that combination, otherwise, no CST exists for the source combination.

2.4. Composition and evaluation of candidate topologies

Following the optimization of individual source combinations, the resulting CSTs are composed into global candidate topologies. Unlike a single CST, candidates may consist of several unconnected sub-networks. Generally, a candidate is formed by any set of CSTs whose underlying source combinations are disjoint.

This includes every individual CST as standalone candidate. Since source combinations represent all subsets of the available heat sources S, ranging from 1 to N, these candidates can cover any number of sources. It is necessary to consider candidates based on subsets because utilizing all available heat sources is not always the most attractive solution. A subset of sources may already supply all lucrative consumers, whereas including additional, expensive sources could make the overall investment package less attractive, even if the total heat supply increases.

Furthermore, candidates are formed by the partitions of source combinations. This is especially relevant if no CST exists for a specific combination of sources. While a combination might be infeasible as a single connected network, it can become profitable if the sources are operated in separate, independent sub-networks. To ensure that the global maximum profit is identified we construct all partitions for every subset of the available heat sources. Since the CSTs for all individual source combinations have already been optimized in the previous step, the composition process simply requires aggregating these pre-calculated results into disjoint sets. A candidate is valid if a CST exists for every source set within its partition.

Finally, global candidate topologies are generated by building the Cartesian product of the candidates from all clusters. Each global candidate consists of exactly one candidate which may itself be a set of sub-networks from each cluster. To determine the final ranking, we evaluate the total profit Π (Eq. (1)) for each global candidate applying for each independent sub-network its local merit order dispatch.

3. Case study and results

This section evaluates the proposed topology optimization framework using the city of Bensheim, Germany with approx. 41,000 inhabitants [14], as a case study. The first sections detail the set up and input parameters of the case study, followed by the presentation of the results.

3.1 Case study description

The initial graph is derived from the 'heat atlas Hessia' [15]. Building geolocations define the consumer nodes and street data the edges. The geographical locations assumed for the source nodes are outlined in Table 1. For clear illustration of the topologies, the outskirts of Bensheim were excluded, leading to an initial graph with 6200 potential consumer nodes. The consumer demands per node are characterized by load profiles generated using standard load profiles by BDEW [16] and building data, including annual heat demand, building type, and age from the heat atlas. For buildings with uncertain age classifications, the most likely age category is selected. Following [17] we assume gradual consumer adoption of DH to account for the remaining lifespan of legacy heating systems, which results in lower initial annual revenues per node. Regarding the edges, the model distinguishes between public network pipes along streets and private pipes connecting buildings to the main grid. To reflect practical investment hurdles and higher attractiveness of large individual consumers, 25% of the private connection costs are allocated to the network supplier.

Source generation profiles are derived from the source peak power $\dot{Q}_s$ and the profile type. While the framework supports detailed profiles, this study adopts constant, step-sequence, and sinusoidal profiles for simplicity. A step sequence is applied to the peak-load boiler that is only available in winter months, while sinusoidal profiles are used for the air-source heat pump (ASHP) and the lake heat pump. These peak in mid- and late July, respectively, with amplitudes derived from source temperature variations and corresponding fluctuations in the coefficient of performance (COP). $\dot{Q}_s$ is estimated based on local spatial constraints and typical technology data. The gas boiler's capacity is limited to a maximum of 10% of the total annual generation at location B. Source investment costs are primarily sourced from *KWW Technology Catalog* [18], which provides data for various unit sizes in Germany. These costs are linearized and annualized $I_s = i_s \cdot Q_{\mathrm{gen},s}(h) + I_{\mathrm{base},s}$ to derive a base cost $I_{\mathrm{base},s}$ and a variable generation dependent cost i_s (Section 2.2). As the catalog provides costs per unit of peak power, these values are converted to be dependent on the generated heat quantity by assuming specific full-load hours (FLH_s) for each source. Following [19], we assume 1,450 FLH for the peak-load boiler and 4,000 FLH for all other units. For simplicity, the interest rate for the pipe network is also applied to the source investments (Table 1). Generation costs for all heat pumps (HP) are based on electricity prices for non-residential consumers [22]. Variable costs further incorporate subsidies from the German Federal Funding for Efficient Heating Networks (BEW) [23], which are adjusted to the pipe lifetime to ensure a consistent annualized comparison:

$$c_{\mathrm{sub,eff}} = c_{\mathrm{sub}} \cdot \frac{1-(1+r)^{-T_{\mathrm{sub}}}}{1-(1+r)^{-T_{\mathrm{topo}}}} = \left(5.5 - \left(6.8 - \frac{17}{SCOP}\right) \cdot 0.75\right) \cdot \frac{1-(1+r)^{-T_{\mathrm{sub}}}}{1-(1+r)^{-T_{\mathrm{topo}}}} \tag{11}$$

Table 1 summarizes the techno-economic characteristics of the seven supply units considered at four locations. Table 2 summarizes the techno-economic parameters applied in all PCST optimizations and Table 3 defines the parameters for the golden ratio search.

Table 1. *Techno-economic parameters of potential heat sources*

Technology	Location*	Peak power $\dot{Q}_s$ [kW]	Variable costs c_s [ct/kWh]	Base cost $I_{\text{base},s}$ [€]	Lifetime [years]	Profile type
ASHP	A	10 000 [20]	7.3 [18]	500 000 [18]	25 [18]	summer peak (amp: 35%)
Sewage plant + HP	B	4 500 [15]	6.4 [18]	180 000 [18]	22 [18]	constant
Lake HP	C	235 [21,22]	8.2 [18]	8 000 000 [18]	25 [18]	summer peak (amp: 25%)
Biomass	C	2 000 [23]	6.5 [24]	0 [18]	28 [18]	constant
Peak load boiler gas	C	400 [25]	9.6 [18]	100 000 [18]	25 [18]	winter (Jan-Mar)
Geothermal borehole + HP	D	70 [26]	13.5 [18]	30 000 [18]	20 [18]	constant
Electric boiler	D	2 000 [19]	22.3 [19]	0 [19]	25 [19]	constant

*Geolocations (lat, lon): A: (49.67182, 8.60325); B: (49.68832, 8.59409); C: (49.68491, 8.60554); D: (49.67337, 8.61124).

Table 2. *Techno-economic parameters PCST*

Parameter	Value	Origin
interest rate r	8%	assumption
network lifetime T_{topo}	50 years	[18]
network efficiency η_{topo}	90%	[27]
pipe cost	1000 €/m	[18]
consumer price p	16 ct.	assumption
initial adoption	50%	[17]
adoption time	10 years	[17]

Table 3. *Algorithmic parameters golden ratio search*

Parameter	Value
max number iterations	20
profit tolerance	0.1%
$\alpha_{\text{min,start}}$	0
$\alpha_{\text{max,start}}$	1

3.2 Results

The following sections present the results, beginning with a comparison of candidate topologies and the identification of the most profitable configuration. Subsequent sections analyze connection pathways across different source locations and an evaluation of computational performance.

3.2.1 Comparison of candidate topologies

The optimization framework identifies one cluster and fourteen valid global candidate topologies for the Bensheim case study. However, not all configurations achieve profitability when base investment costs for the supply units are factored in. All in all, only five candidates are profitable, all of which include only sources at location A and C (Fig 3).

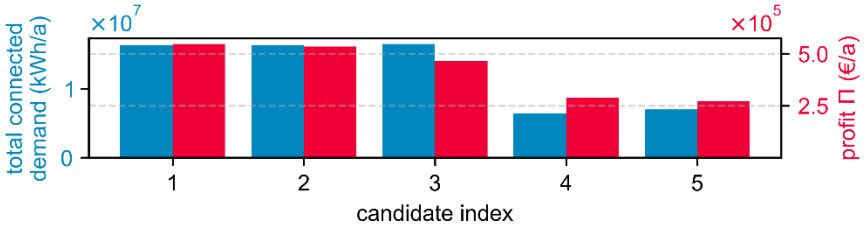

Figure 3. *Connected demand profit of the five profitable networks found by the optimization framework. The candidates are sorted by their profit. Candidate 1 builds ASHP and biomass, candidate 2 additionally the gas boiler. Candidate 3 builds ASHP and gas boiler, candidate 4 biomass and gas boiler, and candidate 5 biomass, gas boiler and ASHP in two separate subnetworks.*

All profitable topologies include at least two sources. Interestingly, the three most profitable candidates connect the same demand of about 16.3 GWh/a as they result in identical network topologies (Fig 4a). The difference in their profits, varying up to 20%, is solely driven by varying source costs highlighting the economic superiority of biomass utilized in candidate 1 over the gas boiler utilized in candidate 3. The ASHP, however, offering the highest peak power, is required in all candidates 1-3 to cover for the connected

demands (Fig 5). Figure 5 illustrates the coverage of demand by different combinations of sources, outlining the shortfall of biomass and gas boiler in capacity. Thus, the topology extends much further as soon as the ASHP is included (Fig 4 (a), (b)). However, as single source the ASHP is not a profitable candidate: in candidate 5 the subnetwork of the ASHP is financed by the surplus of the biomass and gas boiler subnetwork which is why candidate 4 is more profitable than candidate 5. To refinance the high base cost of the ASHP (Table 3) a high demand must be connected, which the ASHP is not capable to cover alone due to missing peak load capacities in winter (Fig 5). This result highlights the benefits of multi-source integration to increase coverage and enabling utilizing renewable energy sources.

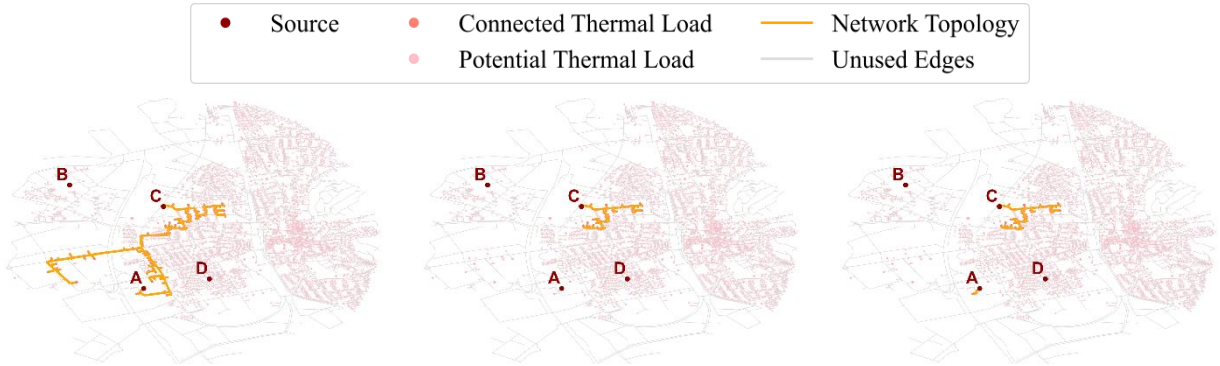

(a) Topology of candidate 1-3 *(b) Topology of candidate 4* *(c) Topology of candidate 5*

Figure 4. *Profitable topologies of case study Bensheim. Candidate 1-3 share the same topology (a). The topologies of candidate 4 (b) and 5 (c) are significantly smaller than the most profitable one (c).*

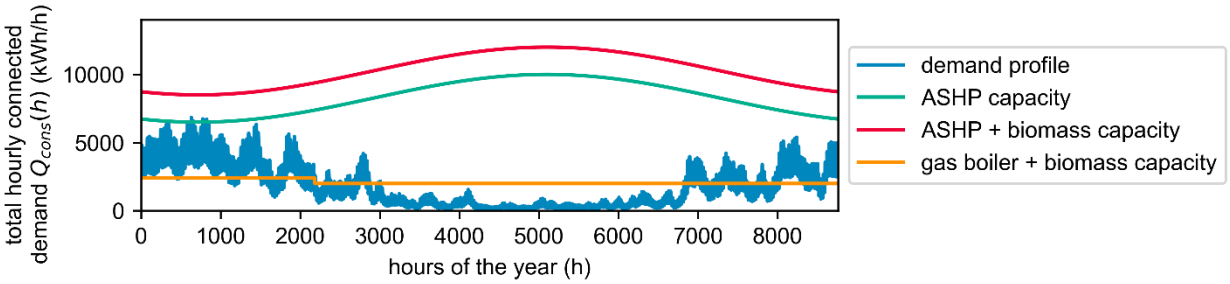

Figure 5. *Coverage of load profile of candidate 1-3 topology by generation profiles. Due to reduced capacity in winter the ASHP cannot cover the heat demand alone. Thus, candidates 1-3 combine multiple sources.*

While profitable configurations center on locations A and C, the framework provides further diagnostic data on the non-profitability of other source combinations. Sewage-based candidates, for example, consistently exceed capacity limits. This indicates that the source's remote location and limited output preclude economic integration with distant high-density demand areas, while local demand remains too sparse for standalone operation. In contrast, geothermal sources fail due to prohibitive variable costs rather than capacity constraints. These insights enable strategic adjustments: planners could augment sewage capacity at Location D with biomass or ASHPs or apply for subsidies to bridge the viability gap of the geothermal option.

3.2.2 Computation time

All simulations were performed on a workstation equipped with a 13th Gen Intel® Core™ i7-13850HX CPU and 32 GB of RAM. The total computation time for the case study Bensheim was 47 minutes. The optimization of source combinations to generate CSTs dominates this runtime. Since the initial clustering resulted in one single cluster, all $2^7 = 127$ source combinations in the set of seven available sources were optimized. In contrast, the subsequent composition and final evaluation of fourteen promising global candidates required only a second, or 0.05 seconds per global candidate. In a hypothetical case where all 127 source combination are feasible, the number of candidates would grow to 4,140 — defined by the Bell numbers as $P_N = B_{N+1} = \sum_{k=0}^{N} \binom{N}{k} B_k$ [28]. Even then the evaluation would still require only 200 seconds, accounting for 7% of the total computation time.

The computational effort required for the optimization of source combinations stems predominantly from the higher complexity of multi-source topology optimization compared to candidate evaluations. Additionally, the total number of required CST optimizations scales exponentially by 2^N with the number of sources N. The computation time of each individual CST optimization scales roughly linearly with the number of sources N_{combi} in the source combination. Notably, converging optimizations are, on average, six times faster than those terminated by the iteration limit (Fig 6). Convergence occurs at an optimum or when the constraints overlap, such that a fragmented topology exceeds capacity limits (Section 2.3.2). The iteration limit is thus only reached when the constraints adjoin without overlapping, which occurs when there is a jump extension from a fragmented to a capacity-exceeding topology with no solution in between. To maintain efficiency as N increases, the proposed framework aims to reduce the number of CSTs through the initial clustering (Section 2.1). However, it is not guaranteed that subclusters can be derived as seen in the case study.

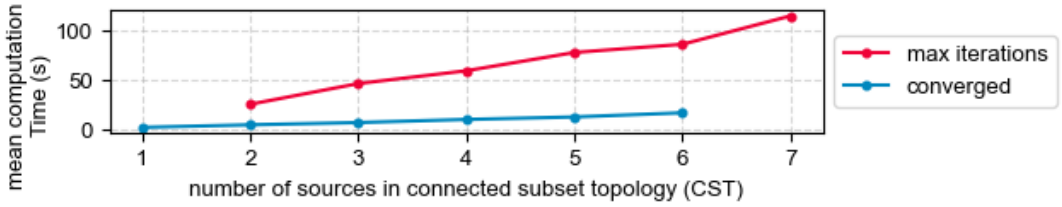

Figure 6. *Mean computation time to optimize a single connected subset topology (CST), differentiated by golden ratio search convergence: converged in < 20 iterations (blue) vs. maximum iterations of 20 (red).*

Nevertheless, the presented framework exceeds the limits of current state-of-the-art models regarding both the number of considered sources and manageable district size. This performance is mainly achieved by the highly efficient underlying PCST approach. Beyond this core efficiency, the framework offers further acceleration potential by parallelizing independent CST computations and by lowering the iteration limit, as the case study demonstrated an upper bound of fourteen iterations for all convergent CSTs. These findings suggest that the method is computationally efficient enough to handle at least 10 sources within a practical timeframe. In a real-world context, the number of potential sources is typically limited by local availability and spatial constraints for renewable technologies. Consequently, the proposed approach is well-suited for most practical district heating planning scenarios.

4. Summary and outlook

The presented work introduces a framework for district heating network (DHN) design that optimizes network topology, source selection, and capacities to maximize economic profitability. By integrating hourly load and generation profiles with geographic data on building level, the method identifies the most profitable combinations of heat sources and consumers, allowing for multi-source topologies that may consist of one or more unconnected subnetworks. To handle multi-source scenarios, the framework generates individual topologies for each source using a prize-collection Steiner tree (PCST) algorithm and joins them into global candidates. The optimal joint topology is derived via a golden ratio search to account for the interdependence of network size, source capacities, and heat supply costs. The total connected demand thereby dictates the generation share of each source based on a merit order principle. The derived candidates are then evaluated based on their annual profit.

Beyond deriving the highest profit DHN, the framework also provides diagnostic value by identifying why specific source configurations are less profitable than others or even fail to achieve economic viability. Such insights allow planners to augment capacities or identify the need for subsidies to bridge financial gaps.

The results highlight that the computational complexity of the problem scales exponentially with the number of sources N, following a complexity of about $O(2^N)$. This inherent challenge has previously limited the scope of such models to 2–3 sources and district sizes of only a few hundred consumers. By leveraging the efficiency of the PCST approach, the proposed framework enables the consideration of up to ten sources in districts with several thousand consumers at the street level for the first time.

To further enhance the framework's computational performance, some refinements offer additional potential: Implementing parallelization offers a path to near-linear scaling of the total runtime, provided suitable computing infrastructure is available. Additionally, stricter clustering heuristics and early stopping

criteria based on convergence analysis could further accelerate the optimization. While the golden search dominates the runtime, the evaluation and comparison stage could be accelerated as well by selectively generating candidates based on their expected economic performance. All these performance gains would facilitate Monte Carlo simulations to quantify uncertainties, such as extreme weather or sudden loss of industrial heat sources, thereby enhancing system resilience.

Regarding the modeling depth, the merit-order approach provides a fast approximation but simplifies source dispatch by presumed full-load hours. Integrating a mixed-integer linear programming (MILP) dispatch layer could refine source sizing and hourly deployment strategies. This enhancement would enable the sophisticated inclusion of thermal storage options. By balancing seasonal and daily fluctuations, storage could mitigate the capacity limitations observed in the standalone air source heat pump (ASHP) configuration of the case study.

Finally, future work should validate the framework against established MILP-based topology models. Although these models are limited in the number of sources they can process, they provide a necessary benchmark for the optimality and accuracy of the presented PCST-based framework.

Acknowledgments

The authors gratefully acknowledge preliminary work by Konstantin Pissarsky and his engagement with this topic in the context of his master's thesis.

This work was supported by the project executing agency Julich (PTJ) with funds provided by the Federal Ministry of Economic Affairs and Climate Actions (BMWK) under Grant No. 03EN3077A.

Nomenclature

Letter symbols

c	variable costs, €/kWh
E	set of edges
FLH	full load hours, h
G	initial graph
h	hour, h
i	annualized variable investment costs, €/kWh
I	annualized investment costs, €
l	length, m
M	big M value
N	number of sources
$OPEX$	operational expenditure, €
p	heat sale price, €/kWh
Q	heat quantity, kWh
$\dot{Q}$	peak power, kW
r	interest rate, -
R	annual revenue, €
S	set of sources
$SCOP$	seasonal coefficient of performance, -
T	lifetime/ investment horizon, years
V	set of nodes

Greek symbols

α	scaling factor, -
η	efficiency, %
Φ	golden ratio
Π	profit, €

Subscripts and superscripts

$'$	solution graph or in solution graph
base	fixed base cost
combi	source combination
cons	heat consumption
const	constant parameter
e	specific graph edge
eff	effective parameter
eval	evaluation value accounting for constraints
gen	heat generation
joint	joint graph from union of sub-graphs
O&M	operations and maintenance
s	specific source
sale	heat sale
sub	subsidy
topo	network topology
v	specific graph node

References

[1] Werner S. International review of district heating and cooling. Energy 2017;137:617–31.

[2] Jodeiri AM, Goldsworthy MJ, Buffa S, et al. Role of sustainable heat sources in transition towards fourth generation district heating – A review. Renew Sustain Energy Rev 2022;158:Art. 112156.

[3] Spirito G, Dénarié A, Fattori F, et al. Assessing district heating potential at large scale: Presentation and application of a spatially-detailed model to optimally match heat sources and demands. Appl Energy 2024;372:Art. 123844.

[4] Marty F, Serra S, Sochard S, et al. Simultaneous optimization of the district heating network topology and the Organic Rankine Cycle sizing of a geothermal plant. Energy 2018;159:1060–74.

[5] Morvaj B, Evins R, Carmeliet J. Optimising urban energy systems: Simultaneous system sizing, operation and district heating network layout. Energy 2016;116:619–36.

[6] Dal Cin E, Carraro G, Volpato G, et al. DOMES: A general optimization method for the integrated design of energy conversion, storage and networks in multi-energy systems. Appl Energy 2025;377:Art. 124702.

[7] Wack Y, Sollich M, Salenbien R, et al. A multi-period topology and design optimization approach for district heating networks. Appl Energy 2024;367:Art. 123380.

[8] Sollich M, Peeters D, Salenbien R, et al. Optimal Placement of Heat Pump Substations in District Heating Networks for Cost-Effective Temperature Reduction. SSRN Electron J 2025. https://ssrn.com/abstract=5901870.

[9] Ceruti A, Lambert J, Spliethoff H. Integrating Renewable Energy and Thermal Storage in District Heating Networks: A Design Optimization Approach. Energy Convers Manag 2025;345:Art. 120323.

[10] Kuper L, Metzger M, Stursberg P, et al. Computationally Efficient Topology Design of District Heating Networks by Price-Collecting Steiner Trees. Energy 2025;333:Art. 137223.

[11] Lambert J, Ceruti A, Spliethoff H. Benchmark of mixed-integer linear programming formulations for district heating network design. Energy 2024;308:Art. 132885.

[12] Johnson DS, Minko M, Phillips S. The Prize Collecting Steiner Tree Problem: Theory and Practice. Proc. Elev. Annu. ACM-SIAM Symp. Discrete Algorithms, San Fransisco, USA: Society for Industrial and Applied Mathematics; 2000, p. 760–9.

[13] Kiefer J. Sequential Minimax Search for a Maximum. Proc Am Math Soc 1953;4:502–6.

[14] Stadtverwaltung Bensheim. Bensheim in Zahlen. Bensheim 2023. https://bensheim.de (accessed December 13, 2024).

[15] LEA Hessen GmbH. Wärmeatlas Hessen 2023. www.waermeatlas-hessen.de (accessed December 13, 2024).

[16] BDEW Bundesverband der Energie- und Wasserwirtschaft e. V. Leitfaden - Abwicklung von Standardlastprofilen Gas. Berlin: BDEW Bundesverband der Energie- und Wasserwirtschaft e. V., Verband kommunaler Unternehmen e. V. (VKU), GEODE – Groupement Européen des entreprises et Organismes de Distribution d'Énergie, EWIV; 2022.

[17] Kuper L, Nouicer M, Stursberg P, et al. A Simulation Framework for District Heating Network Design Capturing Prosumer Decision Making. Proc. 38th Int. Conf. Effic. Cost Optim. Simul. Environ. Impact Energy Syst., 2025, p. In press.

[18] Langreder N, Lettow F, Sahnoun M, et al. Technikkatalog Wärmeplanung 2025. https://www.kww-halle.de/praxis-kommunale-waermewende/bundesgesetz-zur-waermeplanung (accessed March 2, 2026).

[19] Danish Energy Agency. Technology Data Catalogue for Electricity and District Heating Production. 17th ed. Copenhagen: Danish Energy Agency; 2025.

[20] LEA Hessen GmbH. Infoportal für Großwärmepumpen. Infoportal Für Großwärmepumpen n.d. https://grosswaermepumpen-info.de/ (accessed March 23, 2026).

[21] Fink G, Schmid M, Wüest A. Large lakes as sources and sinks of anthropogenic heat: Capacities and limits. Water Resour Res 2014;50:7285–301.

[22] Hessisches Landesamt für Naturschutz, Umwelt und Geologie (HLNUG). Badesee Bensheim. Badeseen Hess 2026. https://badeseen.hlnug.de/ (accessed March 23, 2026).

[23] S2Biom. Tools for biomass chains. S2Biom 2016. https://s2biom.wenr.wur.nl/ (accessed June 23, 2026).

[24] C.A.R.M.E.N. e.V. Marktpreisvergleich - Preisentwicklung bei Heizöl, Erdgas, Holzpellets und Hackschnitzel. CARMEN 2026. https://www.carmen-ev.de/ (accessed March 23, 2026).

[25] Bundesamt für Wirtschaft und Ausfuhrkontrolle. Bundesförderung für effiziente Wärmenetze (BEW). Berlin: Bundesamt für Wirtschaft und Ausfuhrkontrolle (BAFA); 2026.

[26] VDI. VDI 4640 Blatt 2: Thermal use of the underground - Ground source heat pump systems. Berlin: Beuth Verlag; 2019.

[27] Energieeffizienzverband für Wärme, Kälte und KWK e. V. (AGFW), Bundesverband der Energie- und Wasserwirtschaft e. V. (BDEW), Verband kommunaler Unternehmen e. V. (VKU). Fernwärme Preisübersicht. Preistransparenzplattform Fernwärme 2024. https://waermepreise.info/preisuebersicht/ (accessed December 9, 2024).

[28] Aitken AC. A Problem in Combinations. Math Notes 1933;28:xviii–xxiii.